



Title	Hydrogen Content in Arc Atmosphere of Water Curtain Type Underwater Argon Arc Welding
Author(s)	Arata, Yoshiaki; Hamasaki, Masanobu; Sakakibara, Jituo
Citation	Transactions of JWRI. 1981, 10(1), p. 19-25
Version Type	VoR
URL	<a href="https://doi.org/10.18910/7226">https://doi.org/10.18910/7226</a>
rights	
Note	

*The University of Osaka Institutional Knowledge Archive : OUKA*

<https://ir.library.osaka-u.ac.jp/>

The University of Osaka

# Hydrogen Content in Arc Atmosphere of Water Curtain Type Underwater Argon Arc Welding†

Yoshiaki ARATA\*, Masanobu HAMASAKI\*\* and Jitsuo SAKAKIBARA\*\*

## Abstract

The hydrogen content in arc atmosphere in underwater welding was investigated by a direct measurement of the gas just under the arc or by indirect methods such as transfer phenomenon of droplets, generation of blowholes, diffusible hydrogen content and so on. The hydrogen content in arc atmosphere of water curtain type underwater MIG arc welding was estimated about 0.1%.

**KEY WORDS:** (Water curtain type underwater welding) (Hydrogen in arc atmosphere) (Underwater welding Blowhole) (Transferred droplets) (Diffusible hydrogen)

## 1. Introduction

There are some reports on a diffusible hydrogen content in a "wet" underwater welding: manual metal arcs with covered stick electrodes indicate 25-60cc/100g<sup>1)</sup>, which are different from the types of coated materials and a usual CO<sub>2</sub> arc welding with a conventional nozzle indicates 20cc/100g<sup>2)</sup>.

In a water curtain type underwater MIG/CO<sub>2</sub> arc welding, it is thought that the surface of the plate near the arc is shielded perfectly and further the remained water is evaporated by the preheat effect of arc. These mean the partial pressure of hydrogen in arc atmosphere is low, but it is important to declare the partial pressure of hydrogen and the diffusible hydrogen content which affects on the strength of welds.

This report shows the hydrogen content in arc atmosphere by the direct measurement of gas just under the arc or by the indirect measurements such as transfer phenomenon of droplets, generation of blowholes, diffusible hydrogen content and so on.

## 2. Experimental procedure

### 2.1 Observation of preheat effect

It is difficult to observe directly the evaporation of water due to the small bubbles formed with the curtain water in an actual underwater welding. The observation was performed in surface, that is, the TIG arc was generated on the plate which had a 2 mm water film as shown in Fig. 2 and heat input was changed. The shield-

ing gas was pure argon and its flow rate was 20 l/min. A nozzle was 15 mm outer diam. and 10 mm inner diam. and nozzle-base metal distance was 5 mm.

### 2.2 Hydrogen content in arc atmosphere

The gas just under the underwater TIG arc was collected and its hydrogen content was measured. Fig. 1 shows a schematic drawing of gas collecting apparatus used in

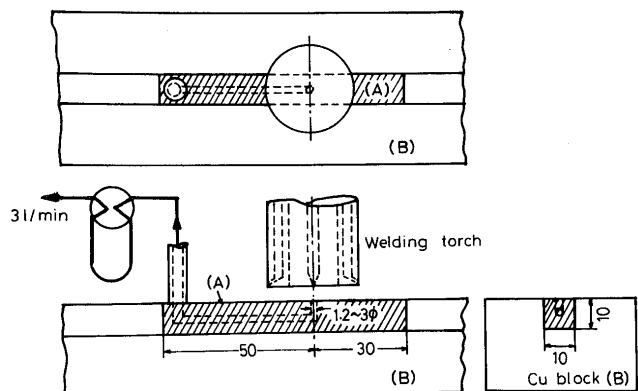


Fig. 1 Schematic drawing of gas sampling apparatus

this experiment, which consists of copper block (A) which has a gas collecting hole of 1.2-3.0 mm  $\phi$ . A tungsten electrode was set just above this hole. This copper block (A) was moved in a groove of 350 mm long copper block (B) together with the torch. The gas in the arc atmosphere was sucked by a vacuum pump at a rate of 3 l/min through

† Received on March 31, 1981

Transactions of JWRI is published by Welding Research Institute of Osaka University, Suita, Osaka, Japan

\* Professor, Director of Research Center for Ultra High Energy Density Heat Source

\*\* Metal and Machine Dep. of Govt.  
Industrial Research Inst., Shikoku

this hole and collected in a glass collector in this pass. The hydrogen in this gas was analyzed with a gaschromatograph.

### 2.3 Critical hydrogen content on blowhole generation

The relation between blowhole generation and hydrogen content in argon as a shielding gas was investigated in surface with the MIG arc welding under spray arc condition. The dual shielding nozzle which had 65 mm  $\phi$ O.D. was adopted and attention was paid to a laminar flow of gas with gas lens to prevent the air contamination. An arc voltage was selected to maintain the constant arc length. The results were arranged based on JIS Z 3104.

### 2.4 Numbers of transferred droplets

The MIG arc welding was performed using a motor generator as a welder. The numbers of transferred droplets in underwater welding were compared with those in surface welding in which the hydrogen was added to argon. The numbers of droplets were searched from the peaks of arc voltage.

### 2.5 Diffusible hydrogen

The diffusible hydrogen in underwater welding was compared with that in surface welding in which the hydrogen was added to argon. It was measured by the glycerine method (JIS Z 3113). The chemical compositions of the plate were shown in Table 1.

Table 1 Chemical compositions of base metal

C	Si	Mn	P	S
0.11	0.19	0.52	0.015	0.016

### 3. Results and discussion

#### 3.1 Preheat effect of arc

In the water curtain type MIG/CO<sub>2</sub> arc welding, in spite of a "wet" welding method, both arc phenomena and bead shapes were similar to those in surface welding<sup>3~5</sup>). But sometimes the blowholes were generated in but welding especially in low heat input because it was

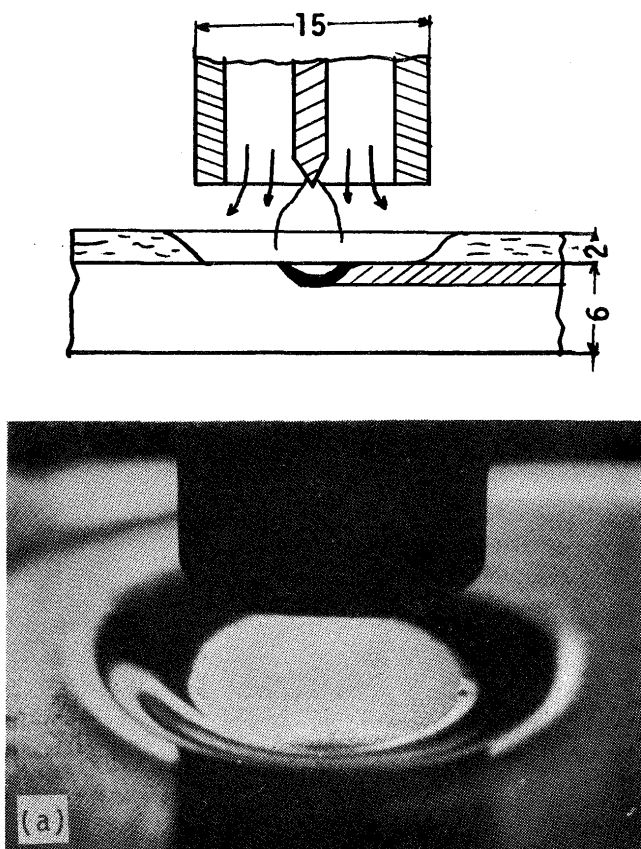


Fig. 2 Sham underwater TIG welding for observation of preheat effect of arc

difficult to remove the water in a root gap and joint phase between works and backing plate. In the same shielding condition, on the other hand, the blowholes were not generated in high heat input<sup>6)</sup>. This may be based on the following consideration: even if the dry region was not obtained and the very thin water film was remained only by the shielding gas, the dry region could be obtained by the preheat effect of arc near the arc spot where the water in front of the arc was evaporated. This dry region may be larger in high heat input.

Fig. 2 (a) shows the condition that the torch is at a standstill and the shielding gas of 20 l/min is flowed out. The water is removed by the shielding gas and a circular region of 13 mm diam. becomes dry condition after the lapse of sufficient time. But when the torch is moved, the thin water film less than 0.5 mm is remained in this region because the fresh water is supplied from the moving direction. Even in this shielding condition, when the arc is generated, the water around the arc is evaporated and dried. Fig. 2 (b) and (c) show the observation results in case the welding current of 120A under welding speed of 25 and 100 cm/min respectively. The region from which the water film of 2 mm is removed becomes small with increasing of welding speed, moreover the very thin water film can be observed in (c). The water film keeps at a distance of 9 mm and 5 mm in front of the arc spot for (b) and (c) respectively, which means that the lower the heat input is, the nearer the water remains and becomes the source of the water vapour.

The evaporation of the water must be contributed to not only the rise of temperature by the heat conduction but also the increase of apparent gas flow rate and heat radiation from the arc column.

The generation of the vapour was notable on the surface of the formed bead which was cooled with the water, but the area was apart from the arc and almost all of the generated vapour was removed with the shielding gas flow to exterior of the arc atmosphere, therefore the arc phenomenon did not affected with this vapour.

### 3.2 Hydrogen content in arc atmosphere

In order to make sure of the decomposition of the water vapour to  $H_2$  and  $O_2$ , the hydrogen content was measured when the arc was generated in the mixed shielding gas of argon and water vapour as shown in Fig. 3. A dew point of this gas was  $-5^\circ C$ , which corresponded to hydrogen content of 0.4%. As the temperature of the arc increases with the current, the decomposition reaction,  $2H_2O \rightarrow 2H_2 + O_2$ , proceeds with increasing of the current. The decomposition rate was 50% in 60A and 65% in 180A.

Fig. 4 and Fig. 5 show the hydrogen content of gas

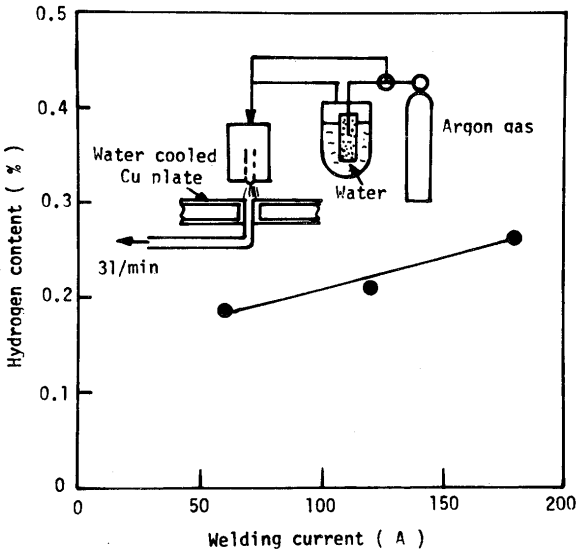


Fig. 3 Effect of current on decomposition of water vapour in argon gas

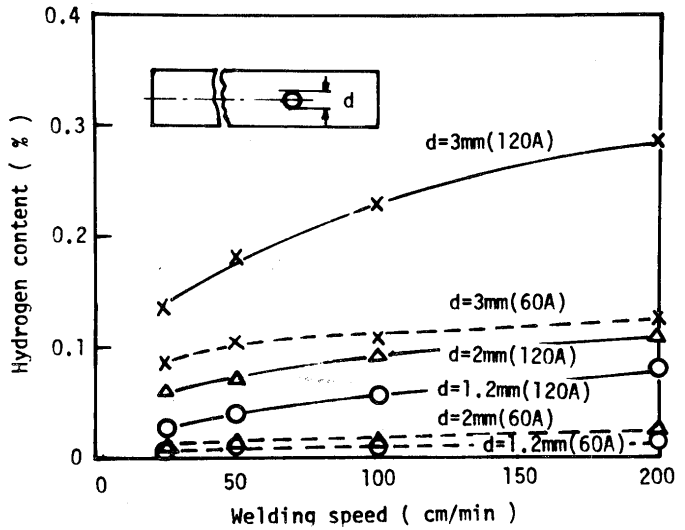


Fig. 4 Effects of current and diameter of gas sampling hole on hydrogen content in arc atmosphere

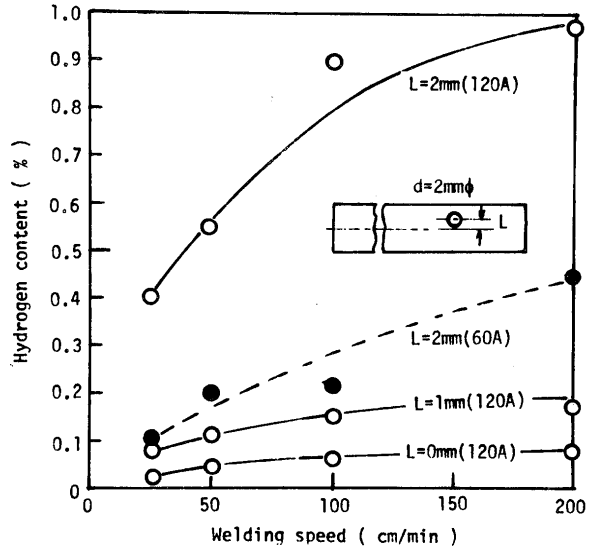


Fig. 5 Effect of position of gas sampling hole on hydrogen content in arc atmosphere

collected with the gas sampling apparatus shown in Fig. 1. Fig. 4 shows the effects of diameter of gas sampling hole and current and Fig. 5 shows the effect of position of sampling hole and current. The copper block moves together with the torch in order to maintain the position of the electrode and sampling hole. The water from the proceeding direction of welding is therefore rather little but it comes from the side through the gap between the two copper blocks, which is different from the actual welding condition. The effect of welding speed was comparatively small due to the above mentioned reason. As the position of the water source did not change, the increase of the current resulted in increase of the evaporation of the water. The effect of the current was therefore larger than that of constant vapour content shown in Fig. 3. The most effective factor was the position of sampling hole and the size of it, that is to say, the distance between arc and water source. The shorter the distance is, the more the hydrogen generates.

The hydrogen content is only about 1% even in case of 120A and  $L = 2$  mm in Fig. 5. The distance between the arc spot and the end of the water film is 5 mm even in the high welding speed of 100 cm/min as shown in Fig. 2. The hydrogen content in an actual welding is therefore supposed to be a condition of 120A,  $L = 0$  mm and  $d = 1.2$  mm in Fig. 5, that indicates 0.08%  $H_2$ .

### 3.3 Critical hydrogen content for generation of blowholes

The generation of blowholes in underwater welding must be caused mainly by the hydrogen gas<sup>7)</sup>. Fig. 6 shows the results of X-ray inspections which show the relation between the amount of  $H_2$  in shielding argon gas and blowholes, that is represented in Fig. 7 based on the JIS Z 3104.

The blowholes generated a little till 15%  $H_2$  except for the starting point and the crater. (If the conventional small nozzle was used, the blowholes generated from 5%  $H_2$ ,

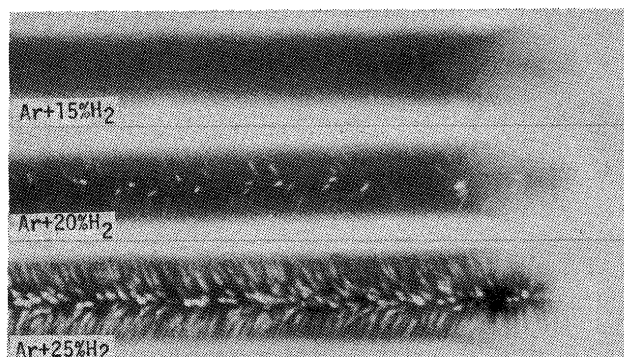


Fig. 6 X-ray inspection results

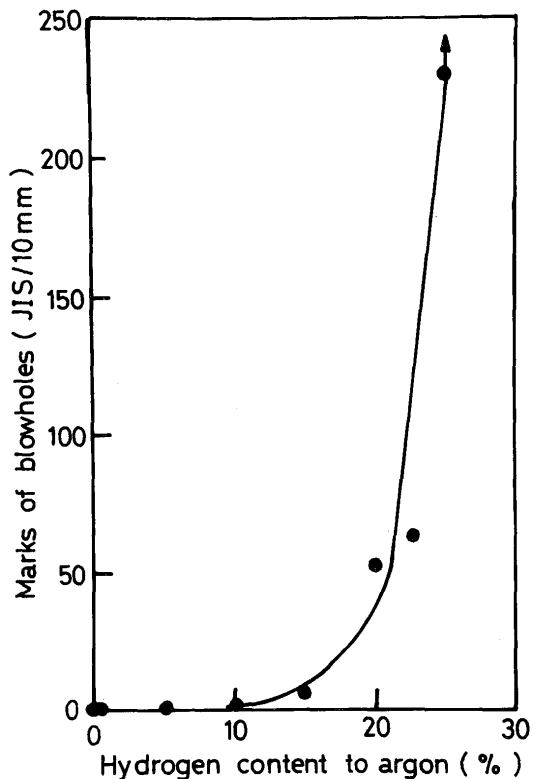


Fig. 7 Effect of hydrogen content in argon on blowholes

which was caused by the air contamination.) On the other hand wormholes coexisted at 20%  $H_2$  and the large amount of wormholes existed at 25%  $H_2$ . The abrupt increase of the blowholes from 20% to 25%  $H_2$  may be related to saturated solubility.

The solubility of the hydrogen to an iron in the equilibrium is shown as follows.<sup>8)</sup>

$$S = \sqrt{P_{H_2} (1 - P_m)} \exp\left(-\frac{\Delta H}{2RT}\right) \quad (1)$$

where  $S$  : equilibrium solubility of hydrogen  
 $P_{H_2}$  : hydrogen partial pressure in atmosphere  
 $P_m$  : metal vapour pressure in atmosphere  
 $\Delta H$  : heat of dissolution  
 $R$  : gas constant  
 $T$  : absolute temperature

The solubility  $S_f$  at a fusion temperature of the iron  $T_f$  is expressed as follows as the metal vapour pressure at  $T_f$  is considered to be zero.

$$S_f = \left[ P_{H_2f} \exp\left(-\frac{\Delta H}{RT_f}\right) \right]^{\frac{1}{2}} \quad (2)$$

At the temperature  $T_{max}$  corresponds to the maxi-

imum solubility of hydrogen, where the metal vapour pressure must be taken into consideration, then write  $S_{\max}$  for the solubility at  $T_{\max}$ , the next equation is given.

$$S_{\max} = [P_{H_2 \max}(1 - P_m) \exp(-\frac{\Delta H}{RT_{\max}})]^{\frac{1}{2}} \quad (3)$$

In order not to generate the blowholes with a supersaturated hydrogen, the solubility of hydrogen at  $T_{\max}$  must be less than that at the maximum solubility at  $T_f$ . So that the critical partial pressure of hydrogen  $P_{H_2 \text{cr}}$  is given when  $S_f$  at  $P_{H_2 f} = 1 \text{ atm}$  and  $S_{\max}$  are equal. Therefore putting  $P_{H_2 f} = 1 \text{ atm}$ ,  $P_{H_2 \max} = P_{H_2 \text{cr}}$  and  $S_f = S_{\max}$  in eq. (2) and (3).

$$P_{H_2 \text{cr}} = \frac{1}{(1 - P_m)} \exp\left[\frac{\Delta H}{R}\left(\frac{1}{T_{\max}} - \frac{1}{T_f}\right)\right] \quad (4)$$

The metal vapour pressure at a high temperature and the temperature for maximum solubility of hydrogen under consideration of the metal vapour pressure are given by D.G.Howden et al, that is,  $T_{\max} = 2400^\circ\text{C}$  and  $P_m = 0.01 \text{ atm}^9$ . If  $\Delta H = 15.6 \text{ kcal/mol}^8$ ,  $R = 1,986 \text{ cal/mol}^\circ\text{K}$  and  $T_f = 1,537^\circ\text{C}$ , then the critical hydrogen pressure is 0.24 atm. This calculated value is agreed fairly with the result shown in Fig. 7 under consideration of false equilibrium caused by a rapid cooling rate in welding.

It was true that a cooling rate in the water curtain type underwater welding was larger than that in surface welding, but it was not affected largely until a solidification temperature because the rapid cooling began from 800-1000°C at which the curtain water struck the bead<sup>10</sup>). If the heat input is the same both in underwater and surface welding, the critical hydrogen content for generating the blowholes must not be much difference. In the water curtain type underwater welding, therefore, the blowholes based on the supersaturated hydrogen can not be generated.

### 3.4 Numbers of transferred droplets

Fig. 8 shows the relation between welding current and numbers of transferred droplets in underwater and surface welding. In a current range of globular transfer, the numbers of droplets in underwater is less than those in surface. But in a spray transfer condition, the difference is not recognized in both cases. The critical current for the spray transfer in underwater becomes a little higher than that of surface (If the critical current is defined as a diameter of the droplet is equal to that of wire (1.6 mmφ only in this case), it is 265A in underwater and 260A in surface respectively).

Fig. 9 shows the relation between hydrogen content in shielding gas of argon and numbers of droplets which is

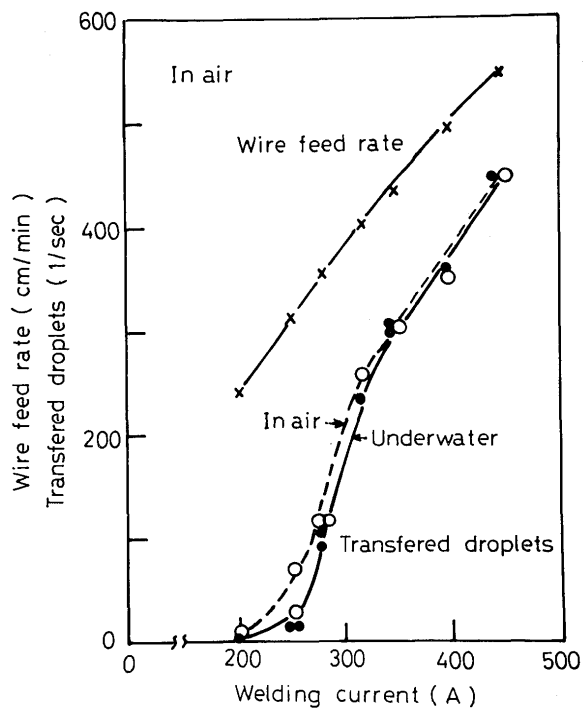


Fig. 8 Relation between welding current and transferred droplets in air and under water welding

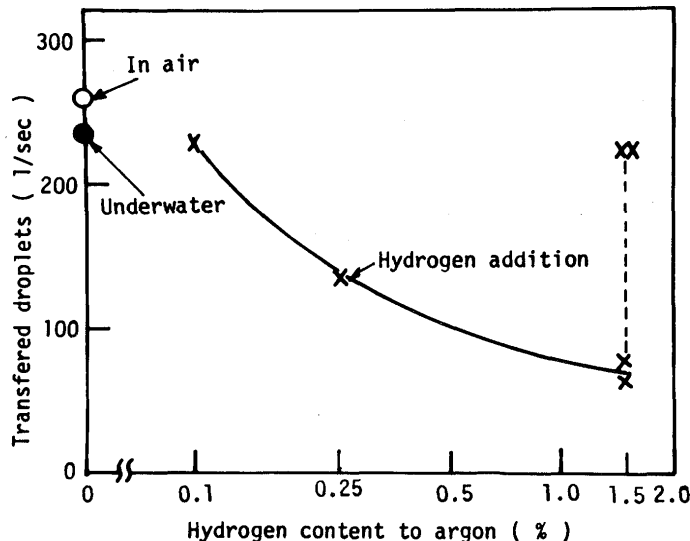


Fig. 9 Relation between hydrogen content in argon and transferred droplets

measured by a oscillogram in a constant welding condition of 29V-320A. The numbers of droplets decreased clearly in 0.25%  $\text{H}_2$ , and the spray or the globular transfer occurred alternately in 1.5%  $\text{H}_2$ .

The hydrogen content in the arc atmosphere in underwater MIG welding can be estimated about 0.1% by comparing the numbers of droplets in underwater and surface.

### 3.5 Diffusible hydrogen in underwater MIG welding

Fig. 10 shows the diffusible hydrogen in the MIG arc welding in surface in which the hydrogen is added to argon as a shielding gas. The abscissa axis is expressed as a

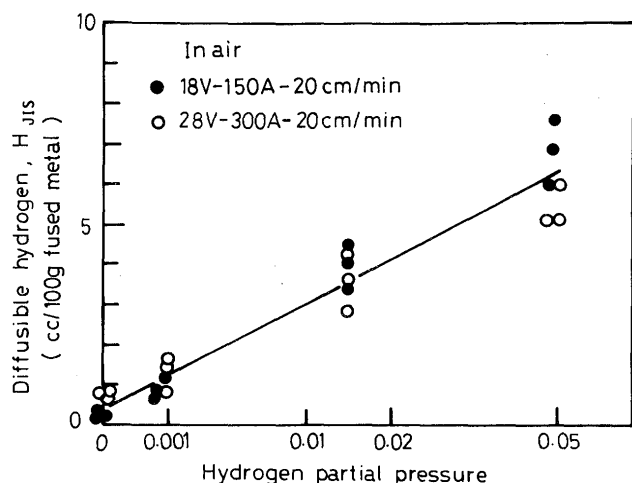


Fig. 10 Relation between hydrogen content in argon and diffusible hydrogen

square root of the hydrogen partial pressure, therefore the diffusible hydrogen is proportional to  $\sqrt{P_{H_2}}$  and agrees with the Sieverts law. But even in case of no hydrogen addition, the diffusible hydrogen less than 1cc/100 g is measured, that is, 0.7cc/100 g for the spray arc and 0.3cc/100 g for the short circuiting arc. This difference based on the welding conditions may be caused by the amount of fused metal.

Taking no account of the difference, the relation between the diffusible hydrogen and the hydrogen partial pressure are described as follows.

$$H_{JIS} = 25.0 \sqrt{P_{H_2}} + 0.5 \text{ cc/100 g} \quad (5)$$

On the other hand, Fig. 11 shows the diffusible hydrogen in underwater welding both in spray and short circuiting arc conditions. In both cases, the data were scattered

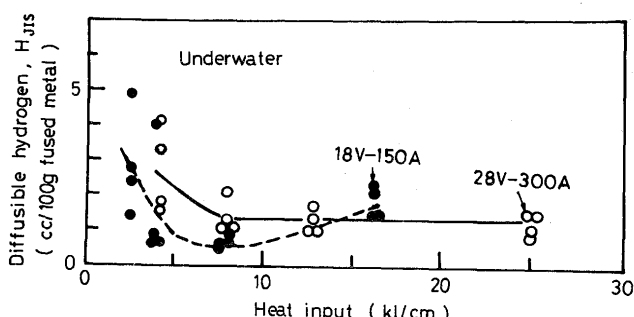


Fig. 11 Diffusible hydrogen in underwater welding

and the hydrogen content increased in the range of a high welding speed and a low heat input. But if the welding speed is too low, as shown in short circuiting arc condition, it had an inclination to increase, which was caused by the formation of a rectangular bead. Therefore it was less than 2cc/100 g in the practical welding speed of 20-40 cm/min. It was 1.1cc/100 g for the short circuiting arc and 1.3cc/100 g for spray arc condition as an average value. Applying these average values to eq. (5), the partial pressure of hydrogen in underwater welding atmosphere was calculated as  $P_{H_2}$  (short) = 0.00058 - 0.058%  $H_2$  and  $P_{H_2}$  (spray) = 0.10%  $H_2$  respectively. The results above mentioned are considered to be overestimated for spray arc and underestimated for short circuiting arc.

The hydrogen absorbed in a fused metal diffuses to a non-fused area or disperses to the exterior from the solidified metal<sup>11)</sup>. The behavior of the hydrogen until the beginning of measuring the diffusible hydrogen is changed by the period of the arc generation (i.e. welding speed) and cooling rate. As the weld metal is cooled rapidly by the water just after the solidification in underwater welding, the hydrogen in the weld metal is apt to be larger than that in surface welding.

From these considerations above mentioned, the hydrogen content in arc atmosphere in underwater welding can be estimated less than 0.1%  $H_2$ .

### 4. Conclusion

Some experiments were performed related to hydrogen content in arc atmosphere. The results are as follows.

- 1) As a source of hydrogen in underwater welding, the thin water film on a base metal was considered and it was shown that the preheat effect by an arc acted effectively upon the evaporation of water in front of the arc.
- 2) The hydrogen content in arc atmosphere measured by a direct and an indirect method was estimated about 0.1% in a range of practical heat input.
- 3) The diffusible hydrogen in the water curtain type underwater MIG arc welding was less than 2cc/100 g ( $H_{JIS}$ ) in practical heat input and this result was better than the other wet welding methods.

### References

- 1) H. Ozaki, T. Naiman and K. Masubuchi, "A Study of Hydrogen Cracking in Underwater Steel Welds", Welding J., 56-8, P231s, 1977.
- 2) H.C. Cotton and D.B.J. Thomas, "Application of Underwater Welding to Offshore Structure", Underwater Const. Tech. Conf., Cardiff, April 1975.

- 3) Y. Arata, M. Hamasaki and J. Sakakibara, "Water Curtain Type Underwater MIG Arc Welding (The 1st Report)", J. of J.W.S., 46-9, P648, 1977.
- 4) Y. Arata, M. Hamasaki and J. Sakakibara, "Water Curtain Type Underwater MIG Arc Welding (The 2nd Report)", J. of J.W.S., 46-10, P278, 1977.
- 5) J. Sakakibara, M. Hamasaki and Y. Arata, "Water Curtain Type Underwater MIG Arc Welding at Water Depth of 200 m", J. of High Temp. Society, 6-6, P244, 1980.
- 6) J. Sakakibara, "Water Curtain Type Underwater CO<sub>2</sub> Arc Welding in Horizontal and Overhead Position", Report of the Govt. Industrial Research Inst., Shikoku, 8-1, P16, 1976.
- 7) I. Masumoto, A. Kondo, Y. Nakashima and K. Matsuda, "Study on the Underwater Welding (Report 2)", J. of J.W.S., 40-8, P748, 1971.
- 8) M. Mizuno, a private message.
- 9) D.G. Howden and D.R. Milner, "Hydrogen Absorption in Arc Welding", British Welding J., 10-6, P304, 1963.
- 10) M. Hamasaki and J. Sakakibara, "Underwater Welding of High Tensile Strength Steel", J. of J.W.S., 48-2, P115, 1979.
- 11) J. Tsuboi, S. Nakano and K. Sato, "The Behavior of Hydrogen in Arc Welding", J. of J.W.S., 42-3, P189, 1973.